blood

Prepublished online April 18, 2013;
doi:10.1182/blood-2012-12-475566

The Thr224Asn mutation in the VPS45 gene is associated with congenital neutropenia and primary myelofibrosis of infancy

Polina Stepensky, Ann Saada, Marianne Cowan, Adi Tabib, Ute Fischer, Yackov Berkun, Hani Saleh, Natasha Simanovsky, Aviram Kogot-Levin, Michael Weintraub, Hamam Ganaiem, Avraham Shaag, Shamir Zenvirt, Arndt Borkhardt, Orly Elpeleg, Nia J. Bryant and Dror Mevorach

Blood (print ISSN 0006-4971, online ISSN 1528-0020), is published weekly by the American Society of Hematology, 2021 L St, NW, Suite 900, Washington DC 20036.

The Thr224Asn mutation in the VPS45 gene is associated with congenital neutropenia and primary myelofibrosis of infancy

Running head: VPS45 neutropenia and myelofibrosis

Polina Stepensky[1]*, Ann Saada[2]*, Marianne Cowan[3], Adi Tabib[4], Ute Fischer[5], Yackov Berkun[6], Hani Saleh[7], Natalia Simanovsky[8], Aviram Kogot-Levin[2], Michael Weintraub[1], Hamam Ganaiem [6], Avraham Shaag[2], Shamir Zenvirt[2], Arndt Borkhardt[5], Orly Elpeleg[2], Nia J. Bryant[3], Dror Mevorach[4].

1. Department of Pediatric Hematology-Oncology, Hadassah, Hebrew University Medical Center, Jerusalem, Israel

2. Monique and Jacques Roboh Department of Genetic Research, Hadassah, Hebrew University Medical Center, Jerusalem, Israel.

3. Institute of Molecular, Cell & Systems Biology, College of Medical, Veterinary and Life Sciences, University of Glasgow, Glasgow, U.K.

4. Rheumatology Research Center and Department of Medicine, Hadassah, Hebrew University Medical Center, Jerusalem, Israel

5. Department of Pediatric Oncology, Hematology and Clinical Immunology, Medical Faculty, Center of Child and Adolescent Health, Heinrich Heine University, Düsseldorf, Germany

6. Department of Pediatrics, Hadassah-Hebrew University Medical Center, Jerusalem, Israel

7. Pediatric Hemato-Oncology Unit, Augusta Victoria Hospital, Jerusalem

8. Department of Radiology, Hadassah-Hebrew University Medical Center, Jerusalem, Israel

* These authors contributed equally to this manuscript

Corresponding authors:

Orly Elpeleg Nia Bryant Dror Mevorach

Elpeleg@hadassah.org.il Nia.Bryant@glasgow.ac.uk Mevorachd@hadassah.org.il

KEY POINTS

- VPS45 is a new gene associated with severe infections and bone marrow failure in infancy that can be treated by BMT.
- The mutation affects intracellular storage and transport and results in increased programmed cell death in neutrophils and bone marrow.

ABSTRACT

Severe congenital neutropenia as well as primary myelofibrosis are rare in infancy. Elucidation of the underlying mechanism is important because it extends our understanding of the more common adult forms of these disorders. Using homozygosity mapping followed by exome sequencing we identified a Thr224Asn mutation in the *VPS45* gene in infants from consanguineous families who suffered from life-threatening neutropenia which was refractory to GCSF, from defective platelet aggregation and myelofibrosis. The mutation segregated in the families, was not present in controls, affected a highly conserved codon and apparently destabilized the Vps45 protein which was reduced in the patients' leukocytes. Introduction of the corresponding mutation into yeast resulted in reduced cellular levels of Vps45 and also of the congnate syntaxin Tlg2 which is required for membrane traffic through the endosomal system. A defect in the endosomal-lysosomal pathway, the homologous system in human, was suggested by the absence of lysosomes in the patients' fibroblasts and by depletion of alpha granules in their platelets. Importantly, accelerated apoptosis was observed in the patients' neutrophils and bone marrow. This is the first report of a Vps45 related disease in human, manifesting by neutropenia, thrombasthenia, myelofibrosis, and progressive bone marrow failure.

INTRODUCTION

Severe congenital neutropenia comprises a group of genetically heterogeneous disorders with a common denominator, an increased susceptibility of neutrophil granulocytes and their precursors to undergo apoptosis[1]. In many of these disorders the bone marrow compartment is depleted, however, the severe congenital neutropenias which are caused by mutations in lysosomal-related genes are characterized by myeloid maturation in the bone marrow.

Primary myelofibrosis is rare in children and the very few patients who presented in infancy originated from consanguineous families, suggesting that congenital myelofibrosis could be transmitted in an autosomal-recessive manner[2,3]. In adults, primary myelofibrosis is characterized by ineffective hematopoiesis and proliferation of dysfunctional megakaryocytes with reticulin and collagen fibrosis in bone marrow, ineffective extramedullary hematopoiesis, and deregulated production of cytokines. The molecular basis in adults includes cytogenetic abnormalities originating at the progenitor cell level or acquisition of the V617F mutation in the JAK2 gene by the hematopoietic stem cell[4,5]. While the JAK2 mutation activates JAK/STAT pathway promoting the transcription of a plethora of proproliferative and antiapoptotic genes[6], the fibrosis likely results from the cross-communication among clonal stem cells which leads to inappropriate cytokine release (reviewed in[7]).

We now report the clinical course and laboratory findings including the results of the molecular investigation in infants originating from consanguineous Palestinian families who presented with life-threatening neutropenia, myelofibrosis and progressive bone marrow failure.

CASE REPORTS

The three index patients, two males and one female, were referred because of recurrent infections since early infancy. They originated from two unrelated Palestinian families and were the products of consanguineous marriages (figure 1). The clinical, hematological and radiological findings of the three index patients and of two older siblings, who were similarly affected but died prior to the study period, are summarized in Table 1. Pregnancy, delivery, birth weight and development during the early neonatal period were uneventful in all the patients. However, between 1-7 months of age they presented with recurrent bacterial infections, typically pneumonia and soft tissue infections. The common pathogens were gram-negative (mainly Pseudomonas) and gram-positive bacteria; invasive fungal infection was documented in one patient. Laboratory investigations disclosed profound neutropenia, progressive normocytic anemia with low reticulocyte count and subsequent development of thrombocytopenia. Peripheral blood smear revealed aniso-and poikylocytosis with teardrop cells, neutropenia and thrombocytopenia with few giant platelets. Hemoglobin F was normal for age. Platelets aggregation was normal with Ristocetin but reduced to 5-28% of the control in the presence of ADP, collagen or epinephrine. Repeated bone marrow aspirations were unsuccessful (dry tap) and biopsy revealed regional acellularity with significant fibrosis. Trilineage hematopoiesis with marked myeloid hyperplasia with maturation and myeloblastic change of the erythroid series was present. Histochemical staining disclosed a significant increase in reticulin fibers. Myelodysplastic syndrome was ruled out and cytogenetic analysis of the bone marrow was normal. Abdominal ultrasound was normal at three months but bilateral nephromegaly with increased parenchymal echogenicity and mild splenomegaly were observed towards the end of the first year of life. Imaging studies revealed diffuse osteosclerosis with striated hyperintense medulla and hyperintense cortex, diffuse sclerotic changes of the diploic space of the skull base and uniformly low intensity of the bone marrow of the pelvis (supplemental figure 1). Four

treated patients had no response to increasing doses up to 30 μg/kg, of GCSF. The oldest among the non-transplanted patients, patient V-5, who was followed until his death at the age of three, had no signs of extra-hematological involvement. Specifically, his cognitive level and communication skills were age-adequate.

The disease run a relentless course and two patients died at 3 months and 3 years, respectively. Two living patients await bone marrow transplantation (BMT) and one patient, V-9, underwent BMT from a matched sibling donor at the age of eight months. Successful engraftment was achieved with full donor chimerism without evidence for graft versus host disease; at three years of age, blood counts were normal and kidney size returned to normal.

Behavioral regression was observed in this patient at 12 months of age, four months post-BMT, and he was later diagnosed with pervasive developmental disorder. Neurological examination, hearing test and brain MRI were normal. No pervasive developmental or any neurological disorders were reported in the other patients.

Molecular investigations performed in patient V-9 revealed no pathogenic mutations in the exons and intronic splice sites of the HAX1, WAS, SBDS, G6PC3 and ELANE genes. The common mutations in JAK2 and BCR/ABL were also excluded.

Of note, the parents and grandparents in families A and B were not aware of any relationship between the two families.

METHODS

LINKAGE ANALYSIS

Homozygous regions were searched in the DNA samples of patients V-4 and V-9 using Affymetrix GeneChip Human Mapping 250K Nsp Array as previously described[8]. The homozygous regions in the patients' samples were identified by inspection. All experiments involving DNA of the patients, their family members and anonymous controls were performed after obtaining written informed consent in accordance with the Declaration of Helsinki and were approved by the Ethical Review Boards of Hadassah and the Israeli Ministry of Health.

WHOLE EXOME SEQUENCING AND BIOINFORMATIC ANALYSIS

The DNA sample of patient V-9 was enriched with Agilent Human V.4 51 Mb Exome Capture kit (Agilent, Santa Clara, CA, USA). Sequencing was carried out on HiSeq2000 (Illumina, San Diego, CA, USA) as 100-bp paired-end runs. Read alignment and variant calling were performed with the October 2011 release of DNAnexus software (Palo Alto, CA) using the default parameters with the human genome assembly hg19 (GRCh37) as reference.

STUDIES IN PATIENTS' CELLS

Cell culture medium consisted of RPMI 1640 (Invitrogen-Gibco, NY) supplemented with L-glutamine and penicillin/streptomycin (Biological Industries, Kibbutz Beit-Haemek, Israel). The APOPTEST-FITC Kit containing Annexin V-FITC was obtained from Nexins Research B.V. (Hoeven, The Netherlands) or from MBL International (Cambridge, MA). Propidium iodide (PI) was from Molecular Probes (Eugene, OR). DiOC6(3) (3,3-dihexyloxacarbocyanine iodide) was purchased from Sigma-Aldrich (St. Louis, MO).

Generation of lymphoblast cell lines.

MNCs were isolated from patient and control donors' peripheral blood. Cells were then transformed with Epstein-Barr virus (EBV) (ATCC, VA, USA) for 1 hour, washed and cultured in RPMI 1640, supplemented with 20% heat-inactivated fetal bovine serum, 2mM L-glutamine, and 1% penicillin/streptomycin antibiotics. Cells were then monitored daily for viability with trypan blue staining and media was replaced once a week. Upon reaching stable cell-division rate, cells were passaged 2-3 times a week.

Western blot of VPS45 protein.

Transformed lymphoblasts from patients and healthy controls were lysed using RIPA lysis buffer (150mM NaCl, 50mM tris pH 8.0, 0.1% SDS, 0.5% Sodium Deoxycholateand 1% Triton X-100, Sigma Aldrich, CA, USA). Total cell lysates were treated with Laemmli sample-buffer, boiled to 85°C degrees for 10 minutes, and electrophoresed through SDS-PAGE 12% separating gel. Proteins were then transferred to a nitro-cellulose membrane (Millipore, MA, USA). The membrane was blocked using 20% skim milk solution (BD, Franklin lakes, NJ, USA). Vps45 and actin were traced using rabbit polyclonal anti- Vps45 antiserum (Synaptic systems, Göttingen, Germany) or mouse monoclonal anti-actin (MP biomedicals, CA, USA), followed by anti–rabbit or anti- mouse IgG horseradish peroxidase (Promega), respectively. Finally, an enhanced chemiluminescence reaction (Biological Industries, Beit Haemek, Israel) was performed and membranes were exposed to UV irradiation and photographed using an LAS3000 imaging system (Fuji).

Neutrophils isolation and culturing.

Blood neutrophils were isolated from fresh blood samples obtained from the patients as described[9]. Constitutive apoptosis was induced by resuspending neutrophils with cell culture

medium and 10% of autologous plasma. Cells were cultured in 24-well plates at 37°C for 4 hours in a humidified incubator containing 5% CO_2.

Apoptosis assessment in leukocytes.

Cell viability was determined by Trypan blue exclusion using a light microscope, at varying times after incubation. Programmed cell death of neutrophils, monocytes, and lymphocytes, was determined in two different ways as described[8]. Phosphatidylserine exposure was determined by measurement of Annexin V- FITC binding, and cells were also stained with propidium iodide (PI) for detection of necrotic cells[8]. Mitochondrial permeability transition was measured as another method for assessment of early apoptosis, based on the ability of intact mitochondria to take up and retain cationic lipophilic fluorescent dyes. To this end, neutrophils were resuspended with 0.3 ml of RPMI and loaded with 1.75 nM DiOC6 for 15 minutes at 37°C. Cells were then transferred to 2-8^{0}C, stained with PI for 10 minutes and analyzed by flow cytometry.

Statistical analysis.

Flow cytometry results were presented as average±SD. The Student's t test was used and differences were considered statistically significant for $p<0.05$.

Apoptosis assessment in bone marrow.

Formalin fixed paraffin embedded bone marrow sections were immunostained for activated caspase 3 (Cell Signaling) using an automated immunostaining system (Benchmark-Ultra, Ventana).

Immunofluorescence analysis.

Sections were deparaffinized and rehydrated by consecutive washes of xylene, ethanol (100% v/v, 95% v/v) and H_2O. For antigen unmasking slides were boiled in 10 mM sodium citrate buffer, pH 6.0, maintained at a sub-boiling temperature for 10 min and cooled at room temperature for 30 min. Sections were washed with H_2O and incubated with blocking solution (PBS, 0.1% Tween-20, 5% normal goat serum) for 1 hr at room temperature. Blocking solution was replaced by primary antibodies (mouse anti-CD177 (clone MEM-166, Abcam, Cambridge, MA) and rabbit anti-cleaved caspase-3 (Asp1775, clone 5A1E, Cell Signaling Technology, Danvers, MA) diluted 1:200 in SignalStain antibody diluent (Cell Signaling Technology) and incubated overnight at 4°C in a humidified chamber. Antibody solution was removed and sections were washed with PBS/0.1% Tween-20. Sections were incubated for 1 h at room temperature in secondary antibodies (chicken anti-rabbit Alexa-488, chicken anti-mouse Alexa 495) diluted 1:1000 in blocking solution. Sections were washed in wash buffer and covered with 4,6-diamidino-2-phenylindole (DAPI)-containing mounting medium (Vectashield, Vector Labs, Burlingame, CA) and coverslips. Digital pictures were captured using an Axiovert 200M microscope (630x magnification) and Axiovision software 4.8.1 (Zeiss, Jena, Germany).

Presence of lysosomes in cultured skin fibroblasts.

Fibroblasts cultured from a skin biopsy of patient V-11 (obtained with informed consent during central line insertion) were maintained in DMEM medium (Biological Industries, Beit Haemek, Israel) containing 4.5 g glucose per liter and supplemented with glutamine and 15% fetal calf serum at 37°C, 5%CO_2. Two days prior to the experiments cells were seeded on glass bottomed 35mm tissue culture plates. The following day, the medium was replaced with the regular medium or with starvation medium as above but with 1% fetal calf serum for 24 hours. Subsequently the fibroblasts were incubated with 50nM lysotracker DND-99

red (Molecular Probes Eugene, Oregon USA) for 30 min where after the medium was replaced with or without 200 nM MitoTracker Green FM (Molecular Probes Eugene, Oregon USA) for 20 min and visualized live by fluorescent confocal microscopy.

Electron microscopy of platelets.

Blood samples were drawn in tubes with citrate as anticoagulant. Platelet-rich plasma (PRP) was prepared by centrifugation at 100 x g for 10 minutes at room temperature. The PRP was fixed with 2% paraformaldehyde and 0.2% glutaraldehyde in 0.1M phosphate buffer pH 7.4 for 2.5 hours and the platelets were stored in 1% paraformaldehyde in phosphate buffer. Subsequently the samples were treated with osmium tetroxide, dehydrated in a graded series of ethanol concentrations and embedded in Epon-Araldite. Sections were stained with uranyl acetate and lead citrate and viewed with a Philips 300 transmission electron microscope.

THE EFFECT OF THE MUTATION IN YEAST

Site directed mutagenesis was used to mutate the 238th codon of yeast VPS45 in the expression construct pCOG070[10] to create plasmid pMC007 (encoding Vps45 harboring the THR238ASN mutation; Vps45T238N). Yeast strains used were SEY6210[11] (containing endogenous Vps45) and a congenic vps45Δ (lacking endogenous Vps45) strain that was constructed by using pNOzY13 to disrupt VPS45 as described[12].

Cellular levels of wild-type Vps45 and Vps45T238N expressed from pCOG070 and pMC007, and endogenous Tlg2 in the same cells, were quantified by densitometry using ImageJ software (NIH) in relation to Pgk1 levels (which was used as a loading control) using immunoblot analysis as described[13].

RESULTS

IDENTIFICATION OF Thr224Asn MUTATION IN THE VPS45 GENE

The search for shared homozygous regions in the DNA samples of the remotely related patients V-4 and V-9 disclosed only one homozygous region larger than 2 Mb, chr1:145243316-158702189 (numbering according to HG19). This region contained 319 protein coding genes, and after *HAX1* was excluded by Sanger sequencing, none of them appeared as an immediate candidate. We therefore opted for whole exome sequencing of patient V-9, which was done at an average depth of x56. This analysis detected a total of 3178 single nucleotide variants (SNVs) and small insertions/deletions (indels) within the targeted coding sequence. We removed those covered less than x7, those present in dbSNP132 or in the in-house database, heterozygous and synonymous variants. Sixty-one changes survived this filtering process but only two of them resided in the shared homozygous region, Chr1:145556666 A>T corresponding to Asp79Val in the ANKRD35 gene and Chr1:150049841 C>A corresponding to c.671 C>A, p.Thr224Asn in the VPS45 gene. Using the pathogenicity prediction software Mutation Taster[14] the ANKRD35 Asp79Val was deemed benign whereas the VPS45 Thr224Asn mutation was predicted pathogenic. VPS45 consists of 15 exons, encoding the 570 residue long human VPS45 protein. Its transcript is most abundant in peripheral blood mononuclear cells and neutrophils[15]. By Sanger sequencing of exon 7 we genotyped the other two patients whose DNA were available, V-1 and V-11, and identified homozygosity for the mutation in both of them. The mutation segregated with the disease in the families (figure 1 and 2A-C). The mutated codon is highly conserved throughout evolution (figure 2D) and the mutation was not found in 120 anonymous individuals of Palestinian origin, nor was it identified in the Exome analyses of 6503 healthy individuals available through the Exome Variant Server, NHLBI GO Exome Sequencing Project (ESP), Seattle, WA (URL: http://evs.gs.washington.edu/EVS/) [12,2012).

FUNCTIONAL CHARACTERIZATION OF THE MUTATION IN YEAST

Vps45 function is best characterized in the yeast Saccharomyces cerevisiae where it regulates the entry of syntaxin Tlg2 into soluble N-ethylmaleimide-sensitive factor attachment protein receptor (SNARE) complexes required for traffic through the endosomal system [12]. Loss of Vps45 function in yeast results in multiple phenotypes including reduced cellular levels of Tlg2[13]. To investigate the effect of the patients' mutation on Vps45 function, we introduced the analogous mutation, Thr238Asn, into the yeast protein and determined the cellular level of Tlg2. This analysis revealed that yeast cells expressing Vps45T238N from a plasmid in place of endogenous Vps45 have reduced cellular levels of Tlg2 by 44.5±9.4% (n=3) compared to cells expressing wild-type Vps45 under the same conditions (Figure 3A). It is important to note that although the two plasmids encoding the wild-type and the Thr238Asn mutant version of Vps45 are identical apart from the mutation of codon 238 (from ACA to AAT), cells harboring the latter have reduced levels of Vps45 by 44.4±7.3% (n=3). Thus, the data presented in figure 3A indicate that the Thr238Asn mutation destabilizes the Vps45 protein thereby abrogates its function in the endosomal pathway.

REDUCED EXPRESSION OF THE MUTANT VPS45 PROTEIN IN PATIENTS CELLS

In order to elucidate the effect of the Thr224Asn mutation on the expression of VPS45 protein, we examined its abundance in lymphoblastic cell lines derived from patients v-4 and v-9. As shown in figure 3B, VPS45 expression was severely reduced in lymphocytes from the patients.

LACK OF LYSOSOMES IN PATIENTS' FIBROBLASTS

Given that mutations in *VPS45* are associated with perturbed trafficking through the endosomal system, we examined the lysosomal compartment in the patients' fibroblasts. In

contrast to control fibroblasts grown in regular medium, lysotracker stain was absent in a patient's cells. Upon starvation, an increase in acidic organelle content was clearly observed in the control cells while barely visible in the patients' cells. In contrast, mitochondrial content visualized by mitotracker green, was unaffected (figure 4A-F).

REDUCED ABUNDANCE OF ALPHA GRANULES IN PATIENTS' PLATELETS

In view of the lysosomes depletion in cultured skin fibroblasts we examined the patients' platelets for the presence of the lysosome-like alpha granules. Transmission electron microscopy of thin section of platelets from the patients disclosed decreased alpha granule content and distorted open channel system (OCS) in comparison with control platelets (Figure 5).

ACCELERATED APOPTOSIS IN PATIENTS' NEUTROPHILS AND BONE MARROW MYELOID CELLS

In order to gain insight into the pathomechanism of Vps45 deficiency, leukocyteapoptosis was evaluated using Annexin-V, PI, and DiOC6 in peripheral blood samples. Bone marrow cells were studied using caspase 3 activation. The results are presented in Table 2 and figures 6 and 7. Patient V-4 showed median fluorescence (MF) of 160±51 of Annexin-V-FITC of which 34±6% were positively gated, whereas controls MF was 68±18 and 21±7% positively gated cells ($p<0.02$, $p<0.05$, respectively, t-test, Table 2). In agreement with these results, 21±14% neutrophils from patient V-4 stained with PI as late apoptotic marker had MF of 923±992 compared with only 3±1% neutrophils with MF of 725±480 in controls (p= non-significant for % gated and $p<0.04$ for MF, t-test, Table 2). Neutrophils from patient V-9 demonstrated MF of 275±16 and 75% of Annexin-V-FITC positive early apoptotic cells ($p<0.0002$, $p<0.0006$, versus controls, respectively, t-test, Table 2) and 5±1% gated cells ($p<0.05$) and MF of 1376±504 ($p<0.05$), for late apoptotic cells. At least two samples from each patient were examined using DiOC6 staining with tight correlation to annexin-V

staining (Figure 6B). When pooled together (table 2) the results were highly significant for both patients indicating higher number of apoptotic neutrophils in patients homozygous for the *VPS45* mutation.

We also compared spontaneous constitutive neutrophil apoptosis[9] following four hours of *in vitro* incubation, in order to observe apoptosis progression. As shown in figure 6C (right), baseline MF of neutrophil Annexin V staining was 145 compared to 51 of control ($p<0.0001$) and four hours later, 274, whereas in control it raised only to MF of 72 ($P<0.004$) (figure 6B). Taken together, the two patients showed accelerated neutrophil apoptosis and accelerated constitutive neutrophil apoptosis indicating that accelerated apoptosis underlies the severe neutropenia observed in these patients. This abnormality was confined to neutrophils as only slightly increased apoptosis was seen in monocytes and no increased apoptosis was seen in lymphocytes (table 2 and figure 6B). In agreement, peripheral blood leukocyte cell numbers were between 1500-5200/μl with nearly normal lymphocyte number 1200-3900/μl and normal to high monocytes number (300-1000/μl), contrasting the severely reduced neutrophil number (100-300/μl) in most CBC. Cell counts following cell isolation showed 50 times reduction in neutrophil numbers as compared to controls but comparable numbers of mononuclear cells.

To assess the presence of apoptosis in the bone marrow, we stained bone marrow sections with an antibody against activated caspase 3. This analysis demonstrated markedly increased apoptosis in the bone marrow (figure 7A-B). We further characterized bone-marrow apoptosis with immunofluorescence staining using DAPI and anti-CD177. The results of this analysis (figure 7C) confirmed increased apoptotic cells in the bone marrow, mainly of the myeloid line.

DISCUSSION

The patients reported in this study presented in early infancy with transfusion-dependent anemia, life threatening thrombocytopenia with significant bleeding tendency and a prolonged, GCSF-resistant neutropenia that caused serious opportunistic infections and led to the death of two of the five patients. The peripheral blood smear was largely abnormal with dacryocytes, nucleated red blood cells and aniso-/poikilocytosis. Rare myelocytes and promyelocytes were present and some platelets were large or unusually shaped. Bone marrow biopsy revealed patchy hematopoiesis with marked fibrosis. Imaging studies invariably showed osteosclerosis with periosteal reaction and nephromegaly which was attributed to extramedulary hematopoeisis. Within the limited follow up period, the disease seemed confined to the hematological system and could be cured by BMT. A longer follow up may be required, as one patient had post-BMT behavioral regression whereas all other patients were neurologically intact.

The parental consanguinity, the presence of the disease in more than one child in each nuclear family and the fact that both sexes were equally affected suggested that this form of infantile myelofibrosis was caused by a founder mutation transmitted in an autosomal recessive manner. The now well accepted combined approach of homozygosity mapping followed by whole exome sequencing resulted in identification of a homozygous missense mutation, Thr224Asn, in the *VPS45* gene. The mutation is most likely pathogenic because this codon is evolutionary conserved, the mutation segregated with the disease in the families and was absent from a large cohort of controls. Pathogenicity was confirmed by the low content of the Vps45 protein in the patients' cells and because the same mutation in Saccharomyces cerevisiae *VPS45* gene resulted in a clear vacuolar protein sorting phenotype which is equivalent to impairment of the endocytic-lysosomal pathway in mammalian cells.

Vps45 is a member of the Sec1/Munc18 (SM) protein family. SM proteins regulate assembly of specific SNARE complexes. SNARE complex formation plays a key role in the specificity of membrane trafficking, bridging opposing lipid bilayers, bringing them into close proximity and providing the energy to mediate their fusion. Vps45 is conserved throughout evolution and by regulating SNARE proteins it is involved in regulating membrane traffic through the endosomal system. Newly synthesized proteins and recycling proteins from the plasma membrane rely on Vps45 for their proper endosomal sorting[16-20]. In yeast, loss of Vps45 function leads to deceleration of cell growth rate, defective endosomal trafficking concomitant with reduced cellular levels of cognate SNARE proteins, increased sensitivity to osmotic stress and accumulation of transport vesicles[13,21]. Similarly, absence of Vps45 in D. melanogaster blocks the fusion of endocytic vesicles into the endosome, resulting in vesicles accumulation and absence of later endocytic structures[22]. Human Vps45 was previously shown to regulate vesicular trafficking between the trans Golgi Network (TGN) and early endosomes and the recycling of plasma membrane receptors[23]. The absence of recognizable lysosomes in our patients' fibroblasts attests to the importance of Vps45 in the biogenesis of the endosomal-lysosomal pathway in humans.

The list of lysosomal related proteins which are associated with congenital neutropenia includes Chediak-Higashi syndrome due to mutations in the lysosomal trafficking regulator (*LYST*) gene, Hermansky-Pudlak syndrome type 2 due to mutations in the *AP3B1* gene encoding the B1 subunit of the adaptor-related protein complex-3, a heterotetrameric complex involved in protein trafficking to specialized endosomal-lysosomal organelles, Griscelli syndrome type 2 due to mutations in *RAB27A*, Cohen syndrome which is associated with mutations in *VPS13B* and a rare form of primary immune deficiency due to a mutation in the endosomal adaptor protein p14 (*ROBLD3/p14*) gene. The exact mechanism underlying the neutropenia in defects of endosomal-lysosomal proteins is unknown.

The accelerated apoptosis observed in our patients' neutrophils could be the consequence of perturbed delivery of cargo from the TGN to the endosomal system which in turn would back-up the earlier secretory pathway. This may lead to an overwhelming ER stress which would trigger apoptosis in a somehow similar way to the sequence of events in patients with congenital neutropenia due to *ELA2* mutations[24,25]. Why neutrophils are more vulnerable than monocytes and lymphocytes is not clear, but may be related to the short life span of neutrophils and the specific pro-apoptotic features of these cells including the unique lack of bcl-2[26]. The large amount of myeloid apoptotic cells in the bone-marrow could also be attributed to their defective clearance reflecting lysosomal dysfunction[27]. Accelerated apoptosis was shown to increase TGF-β secretion[28], and since the TGF-β signaling pathway is a potent negative regulator of proliferation, elevated levels of TGF-β can promote myelofibrosis[29,30]. Whether the accelerated apoptosis observed in Vps45 deficiency enhances TGF-β levels, thereby promoting myelofibrosis, is still a matter of conjecture.

The thrombasthenia seen in our patients may also shed light on the disease mechanism in Vps45 deficiency. In platelets, the endosomal lysosomal pathway is represented by dense core granules, alpha granules and lysosomes, which contain a plethora of bioactive molecules including hemostatic, angiogenic and growth factors as well as proteases, necrotic factors and cytokines. Some of these molecules are produced by megakaryocytes and packaged into granules during biosynthesis. Other cargoes are thought to be endocytosed by circulating platelets and then transported to alpha granules. Impaired granule metabolism manifesting by persistent or intermittent thrombocytopenia or thrombasthenia is common in Chediak-Higashi syndrome and in Hermansky-Pudlak syndrome type 2. In these disorders there is dysfunctional sorting of dense core granule proteins (i.e. serotonin, ADP, polyphosphates) during biogenesis with subsequent loss of cargo from the granules[31]. Gray platelet syndrome due to a defect in an ER protein encoded by *NBEAL2* is unique because in this disorder there is a loss of cargo from alpha-granules[32]. Similar to our patients, the

disease is confined to the hematological system and all the patients have myelofibrosis. We now observe depletion of alpha-granules in our patients' platelets indicating that the Thr224Asn mutation in the *VPS45* gene interferes with the normal alpha granules biosynthesis. Thus, the Vps45 related myelofibrosis could result from a failure of the megakaryocytes to retain synthesized TGF-β, platelet-derived growth factor (PDGF), and fibroblast growth factor (FGF), leading to accelerated apoptosis in the patients' bone marrow.

In summary, we identified the Thr224Asn mutation in *VPS45* in patients with congenital neutropenia, thrombasthenia and myelofibrosis. The precise disease mechanism is currently unclear but the reduced level of the Vps45 protein is associated with accelerated apoptosis in neutrophils and bone marrow, defective alpha-granule biogenesis in platelets and excess of megakaryocytes-derived fibrosing growth factors in bone marrow. This is reflected by the early life threatening bacterial infections with the rapid development of myelofibrosis which can be cured by BMT.

ACKNOWLEDGMENT

The authors are grateful to Prof. Eli Pikarsky for the study of apoptosis in the patients' bone marrow and to Dr. Eduardo Berenstein for assistance with electron microscopy. The excellent technical assistance of Yael Sharir and Rachel Dahan is acknowledged. This work was supported in part by a research grant of the joint fund of the Hebrew University and Hadassah Medical Center to P.S. N.J.B. is a Prize Fellow of the Lister Institute of Preventive Medicine.

CONFLICT OF INTEREST DISCLOSURE

The authors have no conflict of interest to declare

AUTHORSHIP CONTRIBUTIONS

N.S., Y.B., H.S., M.W. and H.G performed clinical identification of patients and wrote a draft of the clinical part of manuscript.

P.S., performed clinical identification and evaluation of patients, data analysis, wrote the clinical section of manuscript and supervised the writing.

A.S. and N.J.B. designed and performed research and data analysis, wrote the research section of manuscript, and supervised the writing.

M.C., A.T., A.K.L., A.Sh., U.F., A.B., and S.Z. performed research and data analysis.

O.E. designed the genetic approach, performed research, data analysis, wrote the research section of manuscript and supervised the writing.

D.M. performed research and data analysis, wrote the research section of manuscript, and supervised the writing.

DATA AVAILABILITY

The CEL file of the SNP array and the exome FASTQ file are available upon request.

REFERENCES

1. Klein C. Congenital neutropenia. *Hematology Am Soc Hematol Educ Program*. 2009:344-350

2. Sieff CA, Malleson P. Familial myelofibrosis. *Arch Dis Child*. 1980;55:888–893.

3. Sheikha A. Fatal familial infantile myelofibrosis. *J Pediatr Hematol Oncol*. 2004;26(3):164-168.

4. Tefferi A. Myelofibrosis with myeloid metaplasia. *N Engl J Med*. 2000;342(17):1255-1265.

5. Campbell PJ, Scott LM, Buck G, et al. Definition of subtypes of essential thrombocythaemia and relation to polycythaemia vera based on JAK2 V617F mutation status: a prospective study. *Lancet* 2005;366:1945-1953

6. Kralovics R, Passamonti F, Buser AS, et al. A gain-of-function mutation of JAK2 in myeloproliferative disorders. *N Engl J Med* 2005;352:1779-1790.

7. Lataillade JJ, Pierre-Louis O, Hasselbalch HC, et al. Does primary myelofibrosis involve a defective stem cell niche? From concept to evidence. *Blood*. 2008;112:3026–3035.

8. Edvardson S, Shaag A, Kolesnikova O, et al. Deleterious mutation in the mitochondrial arginyl-transfer RNA synthetase gene is associated with pontocerebellar hypoplasia. *Am J Hum Genet.* 2007;81(4):857-862.

9. Atallah M, Krispin A, Trahtemberg U, et al. Constitutive neutrophil apoptosis: regulation by cell concentration via S100 A8/9 and the MEK-ERK pathway. *PLoS One*. 2012;7(2):e29333.

10. Carpp LN, Ciufo LF, Shanks SG, Boyd A, Bryant NJ. The Sec1p/Munc18 protein Vps45p binds its cognate SNARE proteins via two distinct modes. *J Cell Biol.* 2006;173(6):927-936.

11. Robinson JS, Klionsky DJ, Banta LM, Emr SD. Protein sorting in Saccharomyces cerevisiae: isolation of mutants defective in the delivery and processing of multiple vacuolar hydrolases. *Mol Cell Biol*. 1988:8:4936–4948.

12. Bryant NJ, James DE. Vps45p stabilizes the syntaxin homologue Tlg2p and positively regulates SNARE complex formation. *EMBO J.* 2001;20:3380-3388.

13. Shanks SG, Carpp LN, Struthers MS, McCann RK, Bryant NJ. The Sec1/Munc18 Protein Vps45 Regulates Cellular Levels of Its SNARE Binding Partners Tlg2 and Snc2 in Saccharomyces cerevisiae. 2012;7(11):e49628.

14. Schwarz JM, Rödelsperger C, Schuelke M, Seelow D. MutationTaster evaluates disease-causing potential of sequence alterations. *Nat Methods.* 2010;7(8):575-576.

15. Rajasekariah P, Eyre HJ, Stanley KK, Walls RS, Sutherland GR. Molecular cloning and characterization of a cDNA encoding the human leucocyte vacuolar protein sorting (h1Vps45). *Int J Biochem Cell Biol*. 1999;31(6):683-694

16. Bryant NJ, Piper RC, Gerrard SR, Stevens TH. Traffic into the prevacuolar/endosomal compartment of Saccharomyces cerevisiae: a VPS45-dependent intracellular route and a VPS45-independent, endocytic route. *Eur J Cell Biol.* 1998;76:43–52.

17. Zouhar J, Rojo E, Bassham DC. AtVPS45 Is a Positive Regulator of the SYP41/SYP61/VTI12 SNARE Complex Involved in Trafficking of Vacuolar Cargo. *Plant Physiol.* 2009;149:1668–1678.

18. Gengyo-Ando K, Kuroyanagi H, Kobayashi T, et al. The SM protein VPS-45 is required for RAB-5-dependent endocytic transport in Caenorhabditis elegans. *EMBO Rep*. 2007;8:152–157.

19. Morrison HA, Dionne H, Rusten TE, et al. Regulation of early endosomal entry by the Drosophila tumor suppressors Rabenosyn and Vps45. *Mol Biol Cell*. 2008;19:4167–4176.

20. Rahajeng J, Caplan S, Naslavsky N. Common and distinct roles for the binding partners Rabenosyn-5 and Vps45 in the regulation of endocytic trafficking in mammalian cells. *Exp Cell Res*. 2010;316(5):859-874 .

21. Piper RC, Whitters EA, Stevens TH. Yeast Vps45p is a Sec1p-like protein required for the consumption of vacuole-targeted, post-Golgi transport vesicles. *Eur J Cell Biol*. 1994;65:305-318.

22. Morrison HA, Dionne H, Rusten TE, Brech A, Fisher WW, Pfeiffer BD, Celniker SE, Stenmark H, Bilder D. Regulation of early endosomal entry by the Drosophila tumor suppressors Rabenosyn and Vps45. *Mol Biol Cell*. 2008;19:4167–4176

23. Rahajeng J, Caplan S, Naslavsky N. Common and distinct roles for the binding partners Rabenosyn-5 and Vps45 in the regulation of endocytic trafficking in mammalian cells. *Exp Cell Res*. 2010 Mar 10;316(5):859-74.

24. Ron D, Walter P. Signal integration in the endoplasmic reticulum unfolded protein response. *Nat Rev Mol Cell Biol*. 2007;8:519–529.

25. Grenda DS, Murakami M, Ghatak J, et al. Mutations of the ELA2 gene found in patients with severe congenital neutropenia induce the unfolded protein response and cellular apoptosis. *Blood*. 2007;110(13):4179–4187

26. Iwai K, Miyawaki T, Takizawa T, et al. Differential expression of bcl-2 and susceptibility to anti-Fas-mediated cell death in peripheral blood lymphocytes, monocytes, and neutrophils. *Blood*. 1994;84:1201–1208.

27. Hsu CL, Lin W, Seshasayee D, et al. Equilibrative nucleoside transporter 3 deficiency perturbs lysosome function and macrophage homeostasis. *Science*. 2012;335:89-92.

28. Huynh ML, Fadok VA, Henson PM. PhosphatidylserIne-dependent ingestion of apoptotic cells promotes TGF-beta1 secretion and the resolution of inflammation. *J Clin Invest*. 2002;109(1):41-50.

29. Dong M, Blobe GC. Role of transforming growth factor-β in hematologic malignancies. *Blood*. 2006;107:4589–4596.

30. Walkley CR, Shea JM, Sims NA, Purton LE, Orkin SH. Rb regulates interactions between hematopoietic stem cells and their bone marrow microenvironment. *Cell*. 2007;129(6): 1081–1095.

31. Huizing M, Anikster Y, Gahl WA. Hermansky-Pudlak syndrome and Chediak-Higashi syndrome: disorders of vesicle formation and trafficking. Thromb Haemost. 2001;86(1):233-245.

32. Gunay-Aygun M, Falik-Zaccai TC, Vilboux T, et al. NBEAL2 is mutated in gray platelet syndrome and is required for biogenesis of platelet alpha-granules. Nat Genet. 2011;43(8):732-734.

TABLE 1: Patients' clinical and laboratory findings

Patient	V-1	V-4	V-5	V-9	V-11
Age at clinical presentation (months)	5	7	5	1	5
Main clinical findings at presentation	Omphalitis, gluteal abscess, lymphadenopathy	Gluteal abscess (Staph. aureus), osteomyelitis	Intra-abdominal abscess	Recurrent infections (gram negative and gram positive), splenomegaly, lymphadenopathy	Recurrent infections (Pseudomonas), splenomegaly, osteomyelitis, invasive fungal infection
Hemoglobin level (g/dl) at presentation	7.3	7.4	8.6	7.7	8.2
Hemoglobin F (%)	N/A	1	N/A	2.8	3.2
MCV, at presentation	84	82	84	86	83
Hemoglobin level (g/dl) range	5-13.2	6.4-10	5-9	6-8.2	6.4-7.8
Absolute neutrophil count(10^9/L) at presentation	100	200	100	250	300
Absolute neutrophil count range (10^9/L)	< 100-1000	< 100-2100	100	< 100-800	< 100-800
Platelets (10^9/L) at presentation	260.0	164.0	56.0	32.0	230.0
Platelets range (10^9/L)	30.0-274.0	6.0-170.0	12.0-96.0	9.0-110.0	180.0-417.0
Peripheral blood smear	N/A	Aniso-/poikilocytosis, dakryocytes, bands	N/A	Aniso-/poikilocytosis, dakryocytes, bands	Aniso-/poikilocytosis, dakryocytes, bands
Bone marrow aspiration	Dry tap	Dry tap	N/A	Dry tap	Dry tap
Bone marrow biopsy	Hypercellularity with myeloid hyperplasia, significant fibrosis	Myeloid hyperplasia, increase of reticulin fibers, fibrosis	N/A	Significant collagenous fibrosis with increased reticulin fibers, left shift and decreased number of megakaryocytes	Myeloid hyperplasia with significant myelofibrosis
Radiological findings	Nephromegaly	Nephromegaly,	N/A	Nephromegaly, sclerotic	Nephromegaly, sclerotic changes

		periosteal reaction, osteosclerosis, absence of diploic space. Resolved after BMT,		changes of the diploic space of skull	of the diploic space of skull
Time to follow up and clinical outcome	Died of sepsis at the age of 3 years	2 years after BMT,100% donor, normal blood count, PDD	Died one week after presentation	18 months, listed for BMT	8 months, treated for invasive fungal infection, listed for BMT

TABLE 2. Early and late apoptosis in leukocytes. Freshly isolated neutrophils, monocytes, and lymphocytes were evaluated for early apoptosis (Annexin+PI-), or late apoptosis (PI+). NA=not applicable, MF= Mean fluorescence, PI= Propidium iodide.

Cells	Viability	Control (n=10)		Patient V4 (n=2)		P value Patient V4		Patient V9 (n=4)		P value Patient V9		Patients V4+V9 (n=6)		P value V4+V9	
		% gated	MF	% gated	MF	% gated	MF	% gated	MF	% gated	MF	% gated	MF	% gated	MF
Neutrophils	Viable cells	76± 8	NA	44± 8.6	NA	0.0324	NA	21± 5	NA	0.0007	NA	28± 14	NA	0.0002	NA
	Early Apoptotic cells	21± 7	68± 18	34± 6	160± 51	0.0525	0.0668	75± 4	275± 16	0.0006	0.0002	66± 23	237± 69	0.0081	0.0009
	Late apoptotic cells	3± 1	725± 480	21± 15	923± 992	0.0960	0.0405	5± 1	1376± 504	0.0431	0.0476	6± 11	1195± 660	0.0456	0.0276
Monocytes	Viable cells	6± 5	NA	28± 7	NA	0.0464	NA	17± 5	NA	0.0264	NA	22± 8	NA	0.0153	NA
	Early Apoptotic cells	91± 6	1839± 782	69± 7	700± 150	0.0960	0.0079	81± 6	1071± 529	0.2676	0.7171	75± 9	886± 383	0.0234	0.0211
	Late apoptotic cells	3± 1	3125± 217	3± 0	4635± 88	0.5527	0.0117	2± 1	3466± 851	0.7196	0.6179	3± 1	4051± 836	0.5503	0.0405
Lymphocyts	Viable cells	68± 15	NA	91±4	NA	0.1204	NA	91± 2	NA	0.2347	NA	91±4	NA	0.0223	NA
	Early Apoptotic cells	31± 15	27± 20	9± 4	21± 8	0.1437	0.4893	9± 2.0	11± 5	0.2418	0.4062	9± 3	16± 8	0.0270	0.3668
	Late apoptotic cells	1± 1	1917± 1023	1± 0	2260± 1524	0.2065	0.8112	1± 1	3747± 664	0.9413	0.0925	0± 0	3004± 1288	0.3097	0.0084

LEGENDS

Figure 1: Pedigree of family A and B. Filled symbols denote affected. Genotype of the c.671 C>A mutation (Thr224Asn) in the VPS45 gene is shown

Figure 2: The Thr224Asn mutation in the VPS45 gene. DNA sequence of part of exon 7 of the human *VPS45* gene in a patient (A), an obligate heterozygote (B) and a healthy control (C). The mutation is shown by the arrow. The conservation of the human Thr224 residue (asterisk) throughout evolution is shown (D).

Figure 3: A. Mutation Thr238Asn in yeast Vps45 (equivalent to Thr224Asn in the human protein) results in lower cellular levels of Vps45 and Tlg2**.** Western blot analysis was used to assess cellular levels of Tlg2 in cells containing (+) or lacking (-) endogenous VPS45. In addition, levels of HA-tagged versions of either wild-type (WT) Vps45 or Vps45T238N (T/N) and Tlg2 were assessed in cells lacking endogenous VPS45 but harboring plasmids pCGO070 (encoding wild-type Vps45) or pMC007 (encoding Vps45T238N). Levels of Pgk1 were assessed as a loading control in all cases. A representative blot of three independent experiments is shown.

B. Western Blot of Vps45 protein. Vps45 was detected by rabbit polyclonal anti-VPS45 antiserum and anti–rabbit IgG horseradish peroxidase followed by an enhanced chemiluminescence reaction. Actin, as a housekeeping gene, is shown at the bottom. Shown are lymphoblasts from two patients and from a normal control.

Figure 4: Depletion of lysosomes in fibroblasts: Control (A-C) and patient V-11 (D-F) fibroblasts were grown in regular medium (A,D) or starvation medium (B,C,E,F) and stained with lysotracker (red) with (C,F) or without (A,B,D,E) subsequent mitotracker (green) stain. Cells were visualized live by fluorescent confocal microscopy without (C,F) or with differential interference contrast (A,B,D,E) at x 400 magnification .

Figure 5: Transmission electron microscopy of platelets. The alpha granule (AG) content is decreased and the open channel system (OCS) is distorted in the patient platelets (A, C) compared to the control cells (B, D) at magnification of x25,000 (A,B) and x8,800 (C, D).

Figure 6: Accelerated apoptosis in patients' neutrophils. A. Freshly isolated neutrophils, monocytes and lymphocytes were stained for Annexin-V expression and Propidium iodide (PI) admission. Mean fluorescence (MF) is indicated for Annexin-V and percentage of PI-positive cells is indicated. A representative example out of samples summarized in Table 2.

B. Mitochondrial permeability transition evaluation in neutrophils. Neutrophils were resuspended with 0.3ml of RPMI and loaded with 1.75 nM DiOC6 for 15 minutes at 37°C. Cells were then transferred to 2-8^{0}C, stained with PI for 10 minutes and analyzed by flow cytometry. Mean fluorescence (MF) and percentage of gated cells are shown. The left lower quadrant includes cells that lost mitochondrial potential (apoptotic cells).

C. Accelerated constitutive spontaneous neutrophil apoptosis. Freshly isolated neutrophils were either immediately evaluated (right) or harvested after 4 h of spontaneous constitutive apoptosis (left). Mean fluorescence (MF) is indicated for Annexin and percentage of PI-positive cells is indicated.

Figure 7. Increased apoptosis in bone marrow. A- Immunostaining of activated caspase 3 in the bone marrow showing markedly increased apoptosis. Representative of three patients.

B. Similarly stained normal bone marrow of a patient of the same age. Biopsy obtained from a patient with Wilms tumor in order to assess the presence of metastases.

C. Increased apoptosis of granulocytes in the bone-marrow of VPS45-mutated patients. Bone marrow sections of a healthy person and three VPS45 mutated patients were

coimmunostained with specific antibodies against activated caspase 3 (green) and CD177 (red). DNA was counterstained using DAPI.

Figure 1

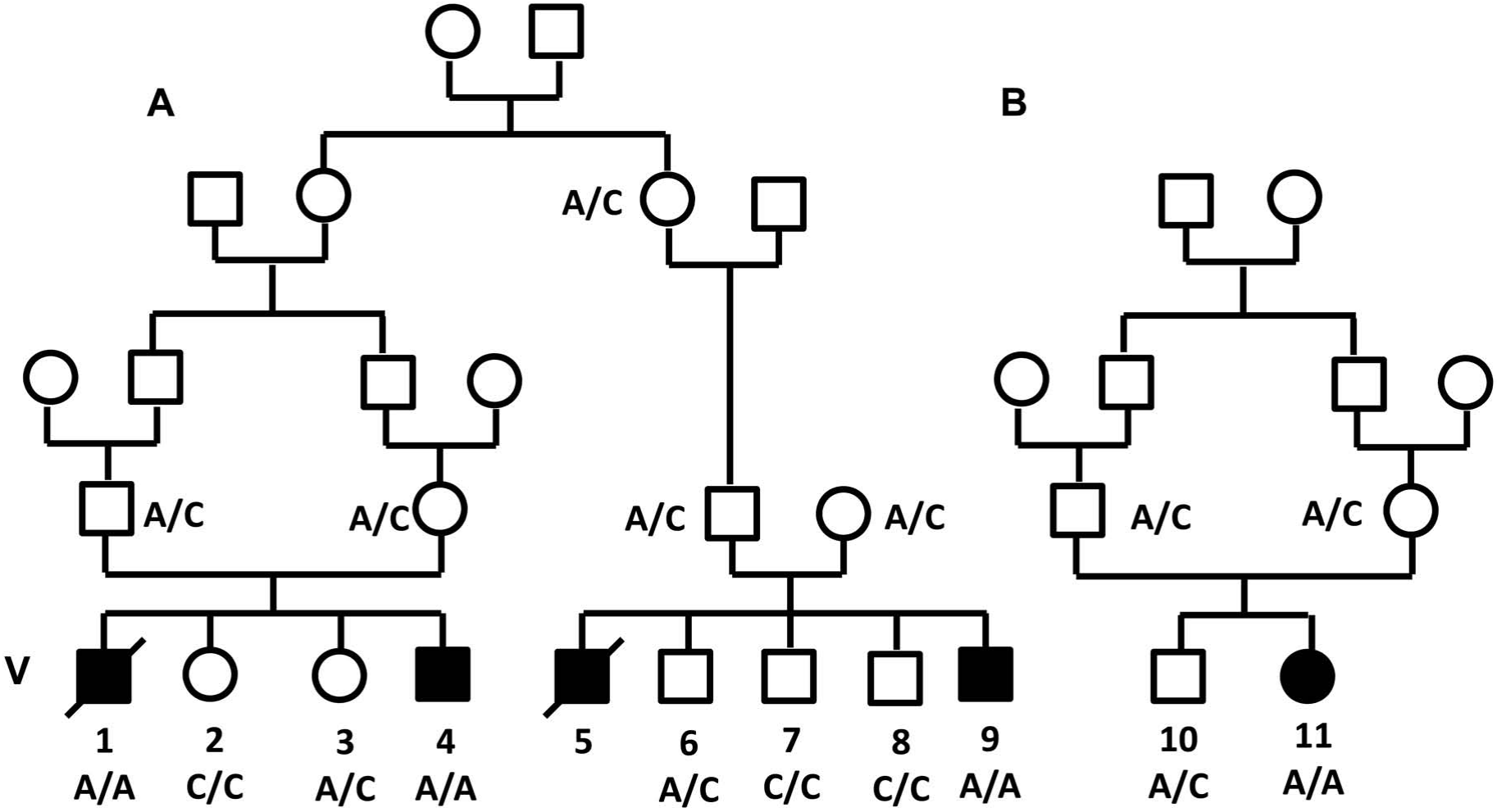
A
B
A/C
A/C
A/C
A/C
A/C
A/C
A/C
V
1
A/A
2
C/C
3
A/C
4
A/A
5
6
A/C
7
C/C
8
C/C
9
A/A
10
A/C
11
A/A

Figure 2

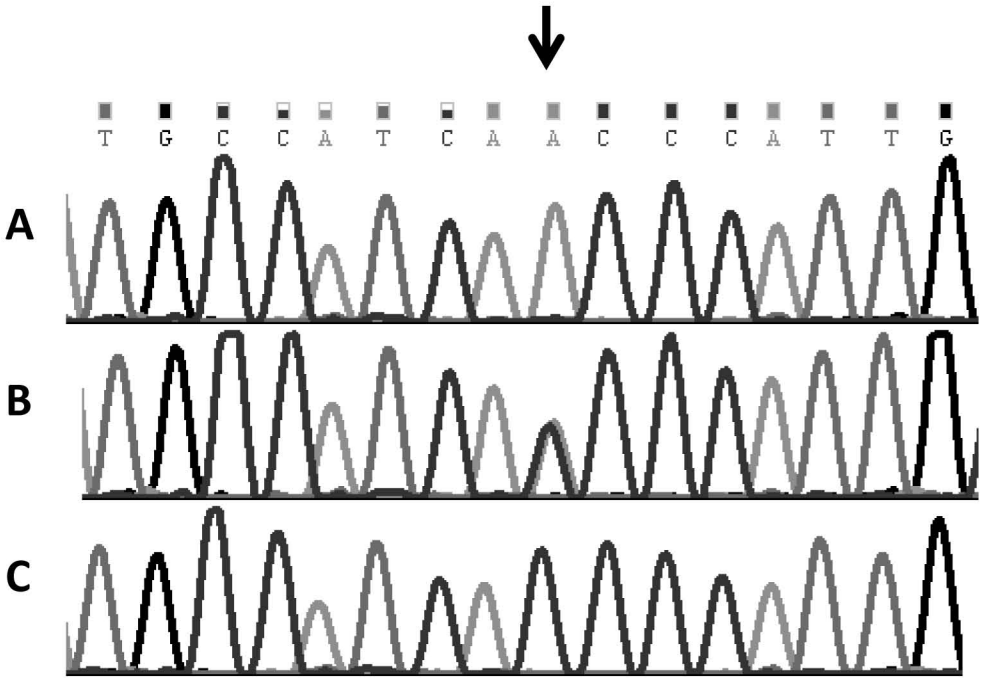

D

				*								
S. Cerviciae	D	P	I	T	P	L	L	Q	P	W	T	Y
A. thaliana	D	P	V	T	P	L	L	N	Q	W	T	Y
C.elegans	D	A	V	T	P	L	L	N	Q	W	T	Y
N.crassa	D	P	I	T	P	L	L	T	Q	W	T	Y
D.rerio	D	A	I	T	P	L	L	N	Q	W	T	Y
human	D	A	I	T	P	L	L	N	Q	W	T	Y
D. Melanogaster	D	P	V	T	P	L	L	H	Q	W	T	Y

Figure 3

A

Endogenous VPS45	+	-	-	-
Plasmid encoding HA-Vps45	-	-	WT	T/N

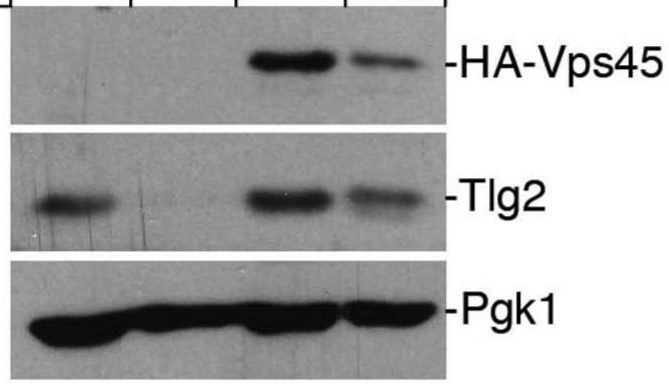

B

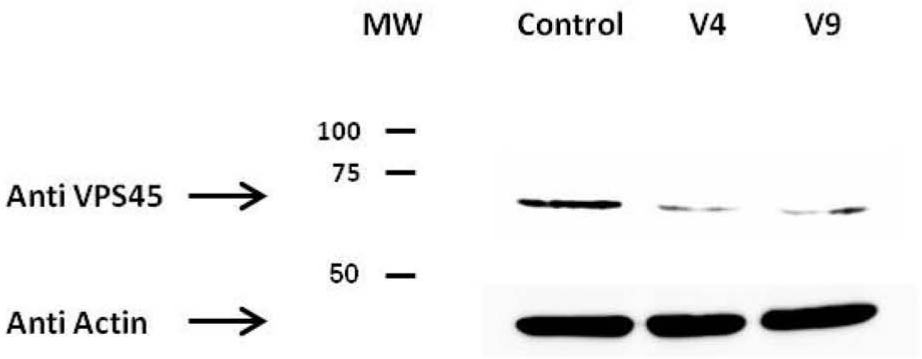

Figure 4

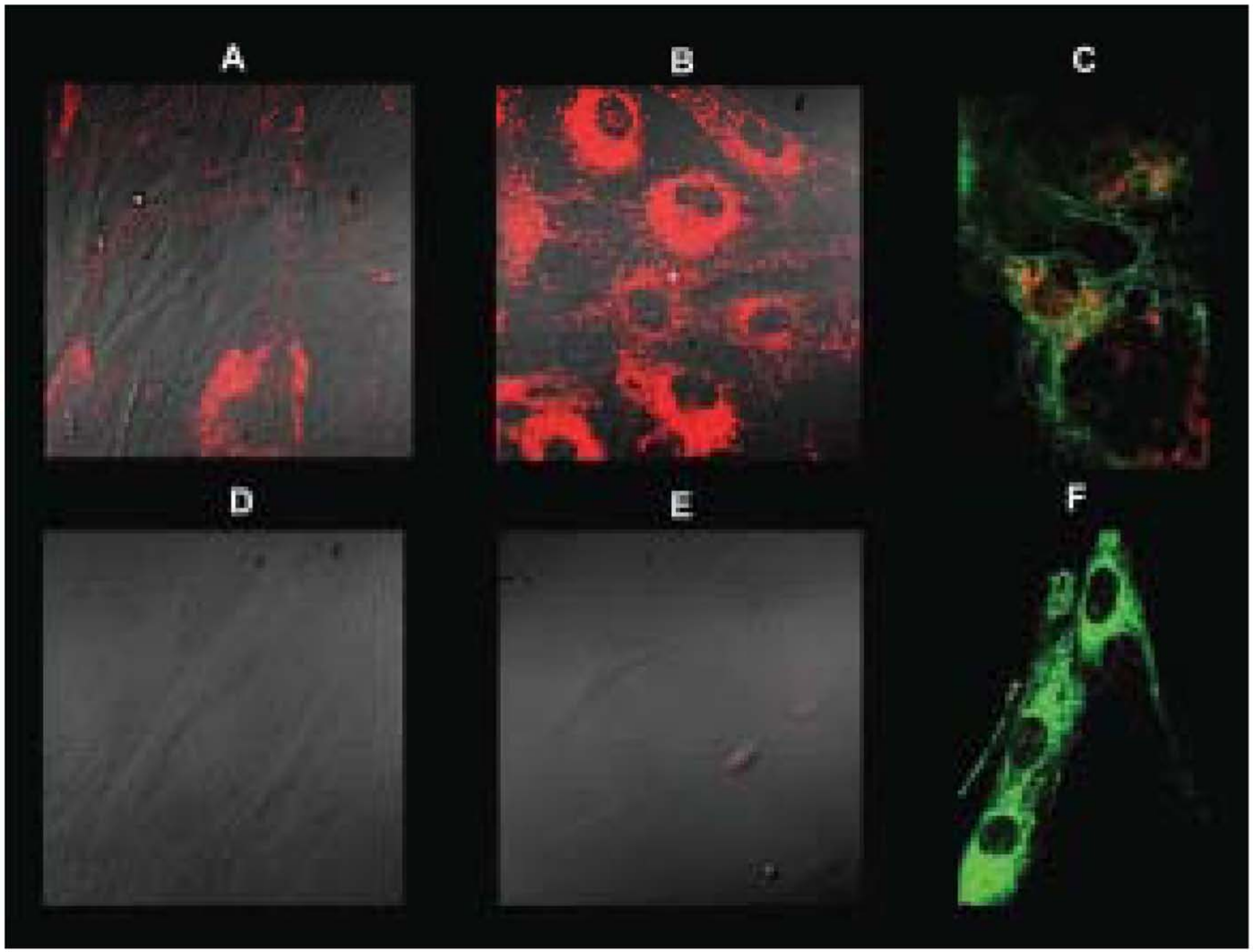

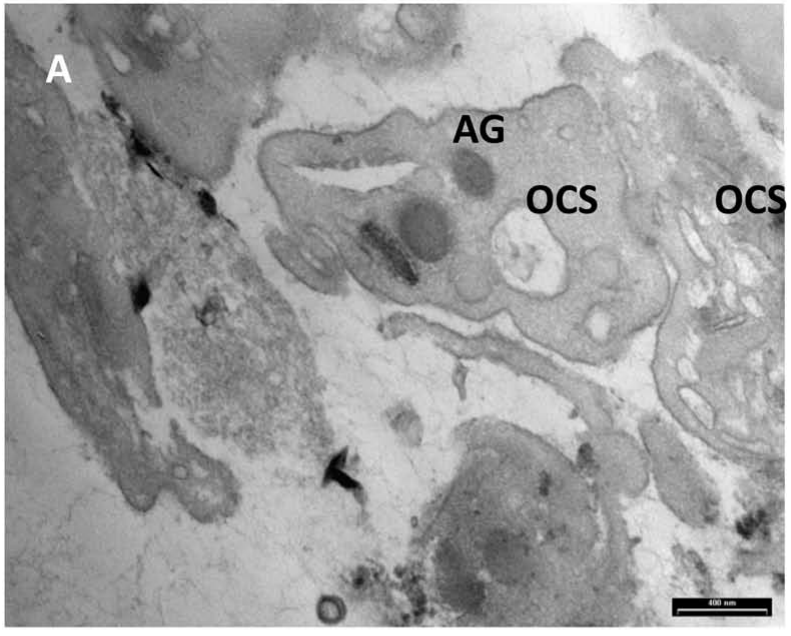

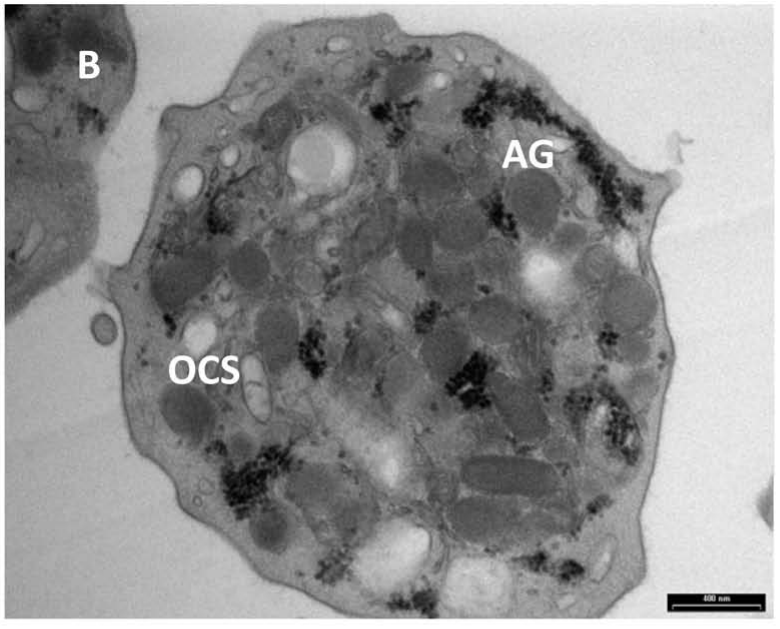

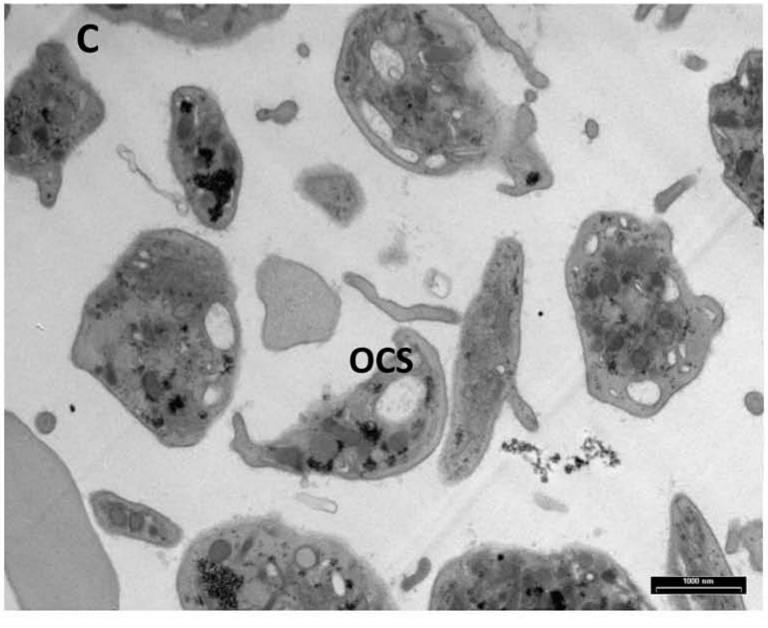

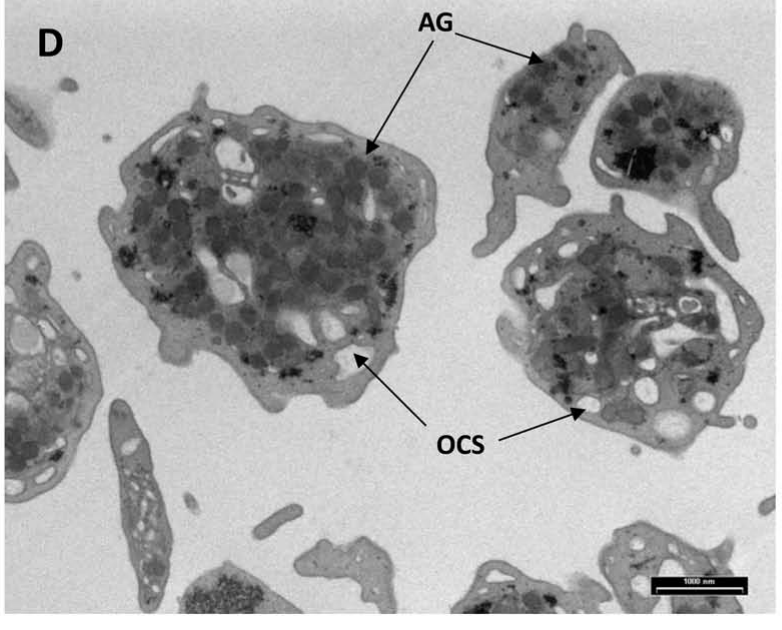

Figure 5

Figure 6A

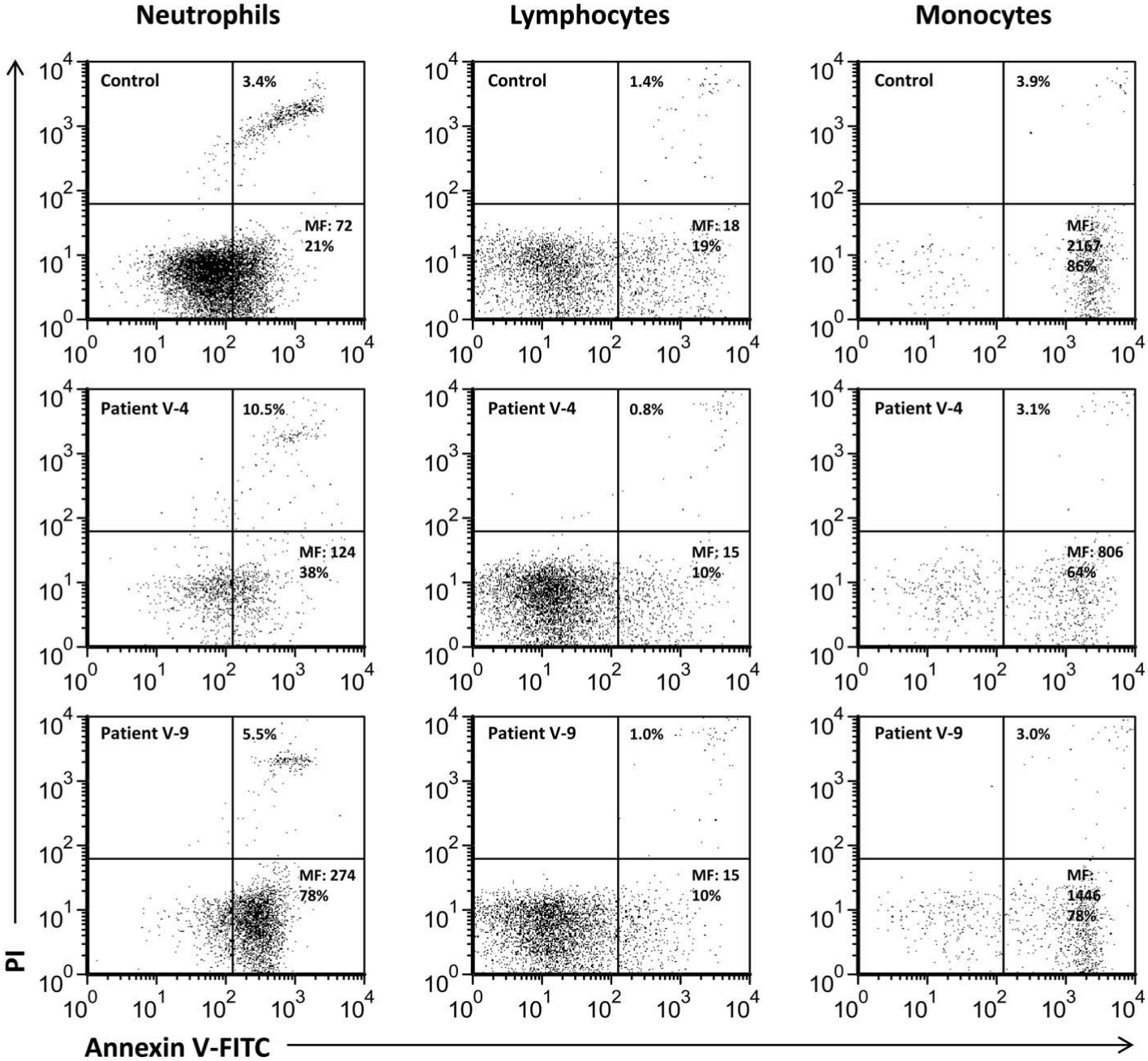
Neutrophils
Lymphocytes
Monocytes
Control
3.4%
MF: 72
21%
Control
1.4%
MF: 18
19%
Control
3.9%
MF:
2167
86%
Patient V-4
10.5%
MF: 124
38%
Patient V-4
0.8%
MF: 15
10%
Patient V-4
3.1%
MF: 806
64%
Patient V-9
5.5%
MF: 274
78%
Patient V-9
1.0%
MF: 15
10%
Patient V-9
3.0%
MF:
1446
78%
PI
Annexin V-FITC

Figure 6B

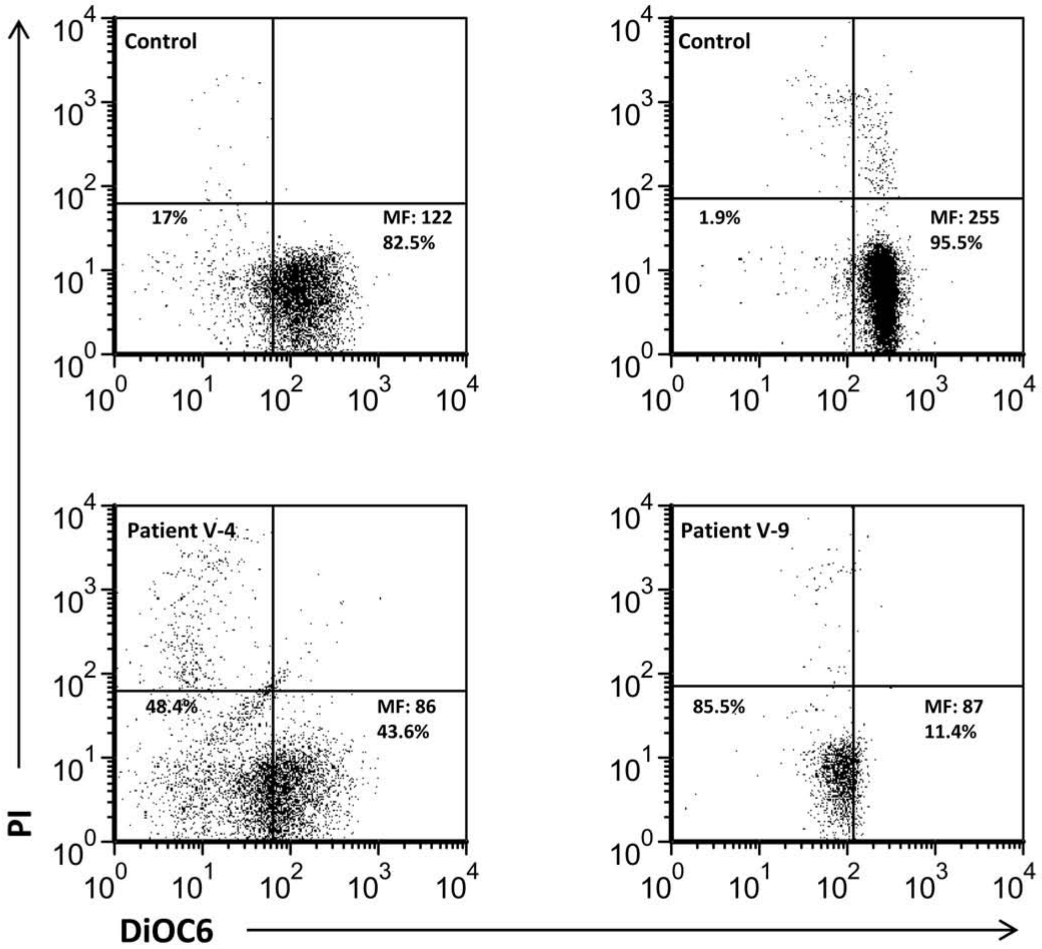
Control
17%
MF: 122
82.5%
Control
1.9%
MF: 255
95.5%
Patient V-4
48.4%
MF: 86
43.6%
Patient V-9
85.5%
MF: 87
11.4%
PI
DiOC6

Figure 6C

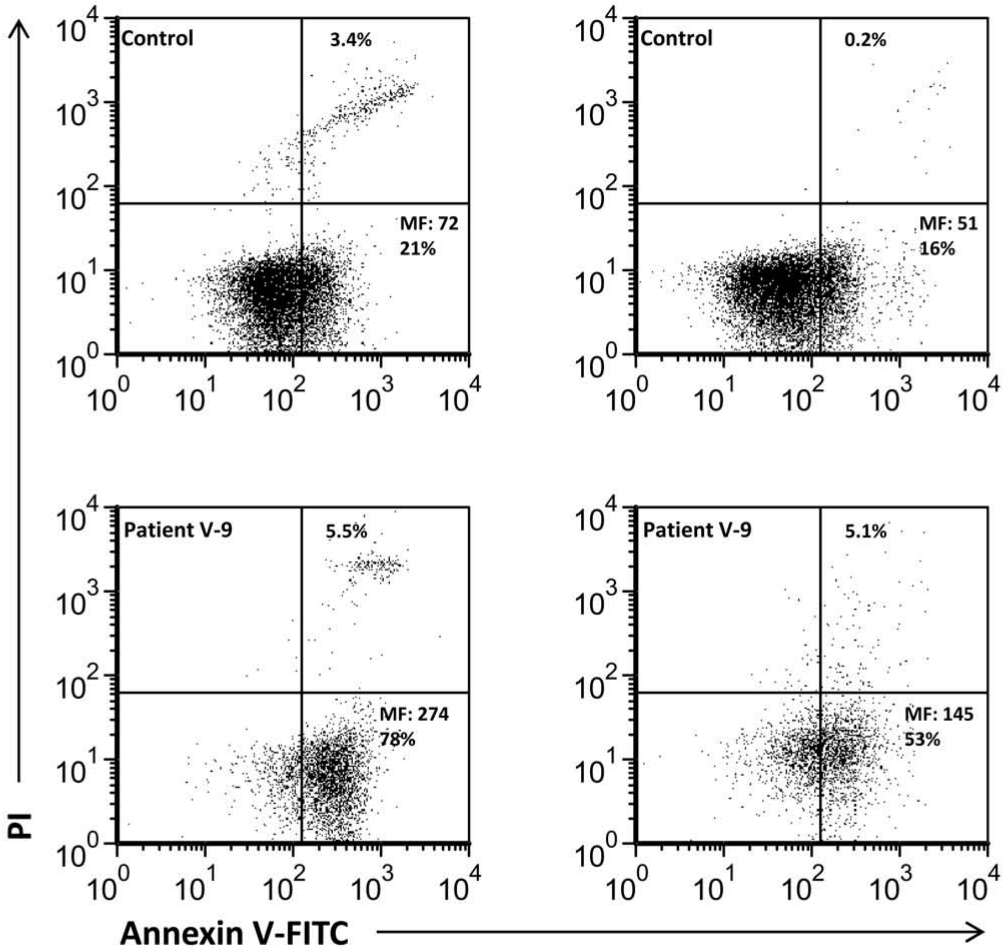
Control
3.4%
MF: 72
21%
Control
0.2%
MF: 51
16%
Patient V-9
5.5%
MF: 274
78%
Patient V-9
5.1%
MF: 145
53%
PI
Annexin V-FITC

Figure 7

A

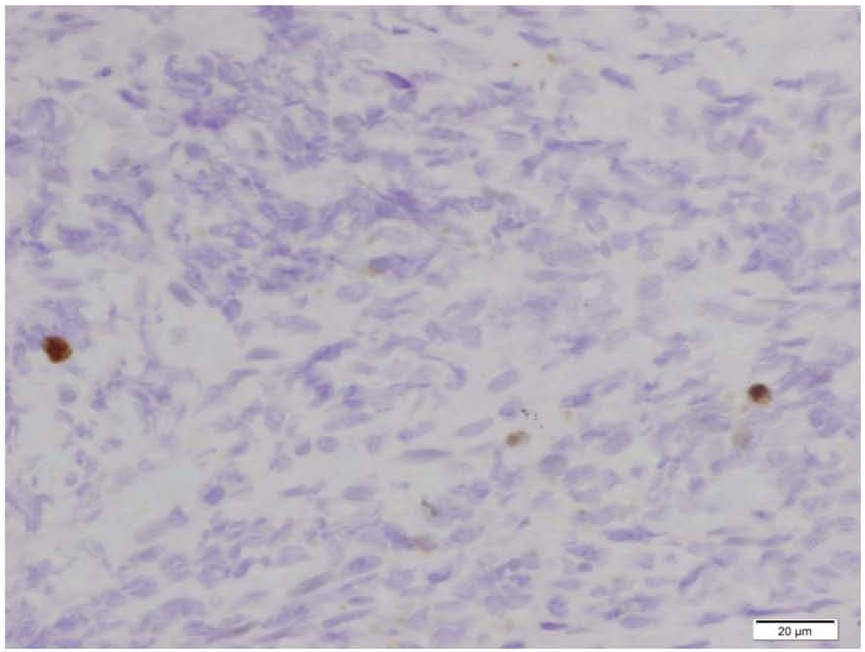

B

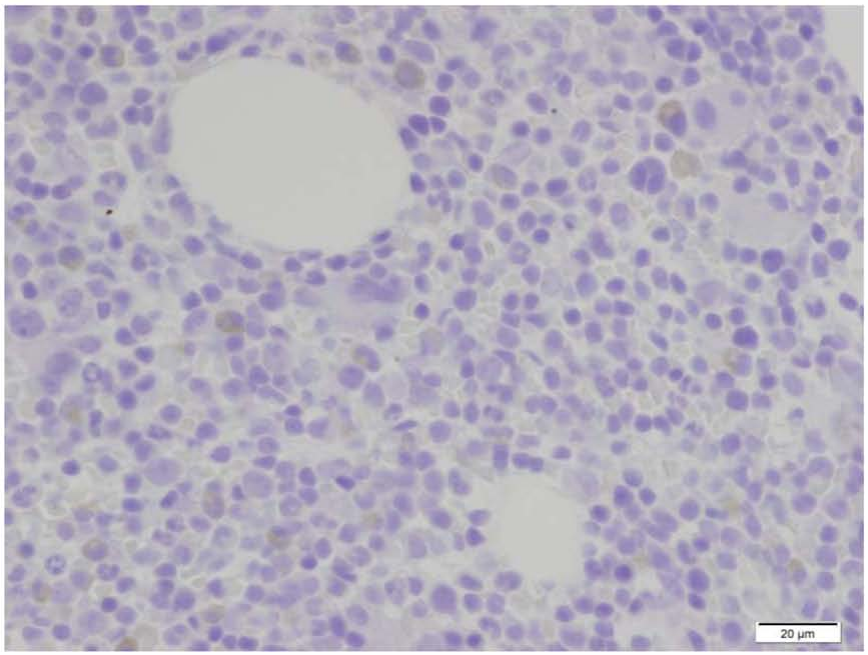

Figure 7C

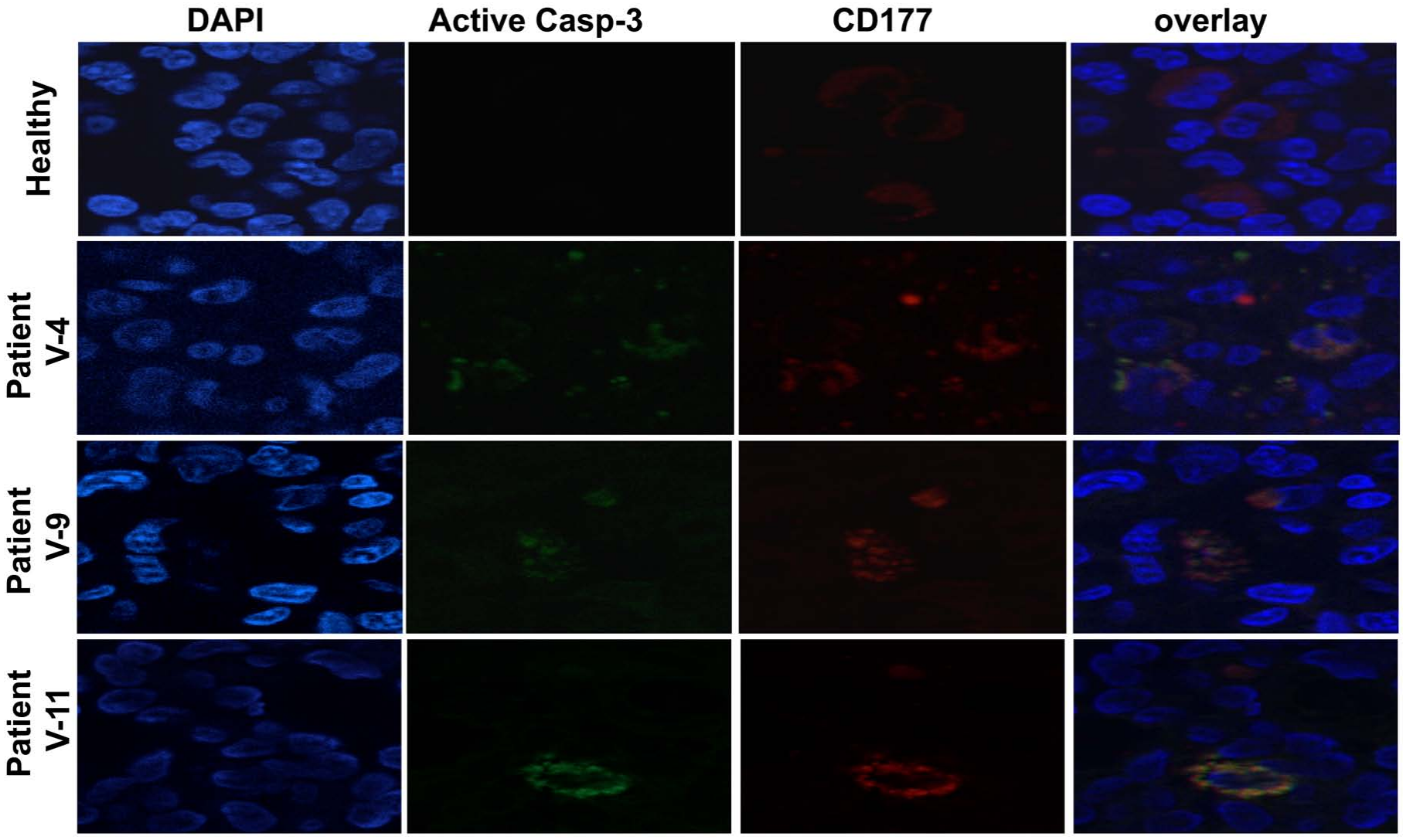
DAPI
Active Casp-3
CD177
overlay
Healthy
Patient V-4
Patient V-9
Patient V-11